Origin of Tensile Stress-Induced Rate Increases in the Photochemical Degradation of Polymers

Rui Chen† and David R. Tyler*

Department of Chemistry, University of Oregon, Eugene, Oregon 97403

Received February 24, 2004; Revised Manuscript Received May 5, 2004

ABSTRACT: A novel poly(vinyl chloride)-based polymer (**1**) containing Mo−Mo bonds along the backbone was prepared by the reaction of carboxylated PVC (ca. 1.8 wt % −COOH) with $(HOCH_2CH_2Cp)_2Mo_2(CO)_6$. When irradiated with visible light, this polymer photodegrades, even in the absence of oxygen. Infrared spectroscopic analysis demonstrated that the chlorine atoms along the polymer backbone act as built-in traps for Mo-centered radicals formed by photolysis of the Mo−Mo bonds. The effect of stress on the degradation quantum yield of **1** and its plasticized analogue (**2**), made by addition of 20 wt % dioctyl phthalate (DOP) to **1**, was studied. The presence of the internal radical trap permitted the polymer samples to be irradiated in the absence of oxygen, thus eliminating the kinetically complicating effects of rate-limiting oxygen diffusion. Results from both polymers showed that stress initially increased the quantum yields for degradation, but the quantum yields reached a maximum value and then decreased with higher stress. These results support the "decreased radical recombination efficiency" (DRRE) hypothesis, one of several hypotheses that have been proposed in the literature to explain the effect of stress on polymer photodegradation rates and efficiencies. The DRRE hypothesis proposes that the function of stress is to increase the initial separation of the photochemically generated radical pair, which has the effect of decreasing their recombination efficiency and thus increasing the degradation efficiency. The hypothesis predicts an eventual downturn in degradation efficiency because of polymer chain ordering; the increased order hinders diffusion apart of the radicals and thus increases their probability of recombination. Wide-angle X-ray diffraction and infrared spectroscopy confirmed that chain orientation increased with increasing stress on polymers **1** and **2**.

Introduction

It is important to understand the photochemical degradation reactions of polymers in order to develop new light stabilizers, to predict the service lifetime of polymers, and to design environmentally friendly degradable materials.[1−4] An interesting outcome of photodegradation studies on polymers is the finding that tensile and shear stress can accelerate the rate of photochemical degradation. For example, recent studies of this phenomenon have shown that tensile stress will accelerate the photodegradation of numerous polyolefins[5−20] as well as polycarbonates,[11] nylon,[21,22] and acrylic−melamine coatings.[23,24] Conversely, compressive stress will generally retard photodegradation reactions.[7] These observations are of enormous practical importance because most polymers are subjected to light and some form of temporary or permanent stress during their lifetime. To control the onset of degradation and the rate of degradation in polymers, it is important to understand the mechanistic origin of the synergism between light and stress in these systems.[25]

Polymers generally photodegrade by a photooxidative pathway involving the autoxidation radical chain mechanism.[26] The photooxidative mechanism, while well-understood, is intricate, involving multiple steps, cross-linking, and side reactions. These features make pinpointing the effects of stress difficult. For example, one formidable complication is that O_2 diffusion can be the rate-limiting step in many photooxidative degradations.[16,27] This adds to the intricacy of the kinetics analysis because O_2 diffusion rates are frequently time-dependent.[27,28] To circumvent these experimental and mechanistic complexities and therefore make it less difficult to interpret data and obtain fundamental insights, we conceived and designed a new class of polymer that photochemically degrades in the absence of oxygen by a relatively straightforward mechanism. The new polymers are based on our polymers that contain metal−metal bonds along their backbones.[25,29−31] Such polymers degrade because the metal−metal bonds are photolyzed by visible light (Scheme 1).[25] As indicated in the scheme, a metal-radical trap must be present for a reaction to occur, otherwise the radicals recombine and no net degradation occurs. Common metal-radical traps include organic halides and molecular oxygen. (Reaction of a metal radical with an organic halide leads to a metal halide and an organic radical (shown generically in eq 1) while reaction with O_2 ultimately leads to metal oxides.) To circumvent the need for O_2 to capture the metal radicals, the polymers used in this study contain built-in radical traps. By eliminating the need for external O_2 to act as a radical trap, the plan was to exclude the complicating kinetics features of diffusion-controlled oxidation reactions.

Scheme 1. Photochemical Degradation of a Polymer with Metal−Metal Bonds along Its Backbone

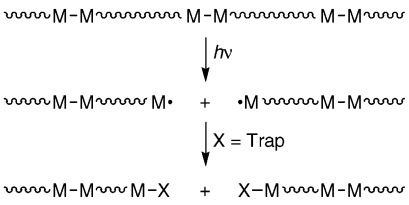

$$L_nM^{\bullet} + R{-}X \rightarrow L_nM{-}X + R^{\bullet} \quad (1)$$

* Corresponding author. E-mail: dtyler@uoregon.edu.
† E-mail: ruichen@darkwing.uoregon.edu.

10.1021/ma0496302 CCC: $27.50 © 2004 American Chemical Society
Published on Web 06/18/2004

In this paper, we report the results of our study on the effects of stress on the photodegradation quantum yields of a poly(vinyl chloride) polymer with Mo−Mo bonds along its backbone. The results are compared to the predictions of three theories that were developed to explain the effects of stress on degradation efficiencies. The experimental results closely match the prediction of one of the theories, and from this result, it is possible to gain mechanistic insight into the origin of stress effects on degradation efficiencies. A portion of this work has appeared as a Communication.[32]

Experimental Section

Materials. Carboxylated poly(vinyl chloride) with carboxyl content 1.8 wt % was obtained from Aldrich and used as received. Thionyl chloride (Fluka, 99%) was stored in a desiccator and used without further purification. Triethylamine (Aldrich, 99.5%) and dioctyl phthalate (DOP) (Aldrich, 99%) were stored in a drybox and used as received. $(HOCH_2CH_2C_5H_4)_2Mo_2(CO)_6$ was prepared as previously described.[29] THF and hexane were refluxed with potassium under N_2 and distilled before use. The dry THF was degassed by at least three freeze−pump−thaw cycles before use.

Instrumentation. Infrared spectra were recorded on a Nicolet Magna 550 FT-IR spectrometer with OMNIC software. The samples of polymeric products were prepared as KBr pellets, as solutions in THF, or as neat polymer films. Two hundred scans were collected for the stressed polymer films. UV−visible spectra were recorded on a HP 8453 spectrophotometer. Glass transition temperatures, T_g, were measured using a Du Pont 2950 thermal analyzer and a heating rate of 10 °C/min. X-ray diffraction measurements were made at room temperature with a Scintag XGEN-4000 generator operated at 40 kV and 20 mA with a Scintag XDS 2000 vertical goniometer. Ni-filtered Cu Kα radiation was used in an air atmosphere. Diffraction patterns over the range 10−50° 2θ were obtained from the flat rectangular cast film of the polymers with weights at both ends of the film. The scanning speed was 0.02° 2θ per second. No correction was made for air scattering. Tensile tests were carried out at room temperature using an Instron mechanical tester at 5 mm/min grip separation speed. Rectangular samples were the same size as those used in the degradation experiments. The stress was calculated using the area of the initial cross section, and the strain was calculated from the displacement of the initial and final grip separation.

Synthesis of Acyl Chloride-Activated PVC. Carboxylated PVC (4 g, 1.47 mmol of −COOH) was dissolved completely in dry THF (300 mL) in a 500 mL Schlenk flask equipped with a condensation tube and a gas absorption tube filled with $CaCl_2$. Thionyl chloride (3 mL, 40.9 mmol) was added dropwise into the solution with stirring. The reaction mixture was refluxed at 70 °C for 36 h. The crude product was condensed to a sticky state by evaporating most of the solvent under reduced pressure. Dry hexane (100 mL) was then added and an off-white product was precipitated. This was separated from the solution by filtration and washed with fresh dry hexane (100 mL ×2). The acyl chloride-activated PVC was then dried in a vacuum (3 days). Yield: 3.2 g; 80%. IR (of thin film): ν(C═O) 1778 (s) and 1730 (m) cm^{-1} (for comparison, the carboxylated poly(vinyl chloride) PVC−*C*OOH has bands at 1772 (m) and 1728 (s) cm^{-1}). UV−vis (in THF): $\lambda_{max} = 361$ nm. $T_g = 88$ °C.

Preparation of Polymer 1. The following manipulations were done in a glovebox under N_2. Acyl chloride-activated PVC (0.4 g, 0.157 mmol −COCl) was dissolved in dry, degassed THF (50 mL) in a 100 mL flask equipped with a magnetic stirring bar. A solution of $(HOCH_2CH_2C_5H_4)_2Mo_2(CO)_6$ (0.045 g, 0.077 mmol) in a small amount of THF was added dropwise into the solution containing the acyl chloride-activated PVC, followed by the addition of triethylamine (1 mL). The reaction was stirred for 2 days before separation. At that time, the solid salt of triethylamine hydrochloride (observed on the wall of the flask) was removed by filtration. The filtrate was concentrated by evaporating half of the solvent. The solution was then poured onto a Teflon-coated pan to cast a film. The film was dried for 2 days in the glovebox and then placed under vacuum to dry it completely. IR (of thin film): ν(C═O) 1770 (s) and 1730 (m) cm^{-1}; ν(C≡O) of $[-Mo_2(CO)_6]$, 2005 (m), 1950 s, and 1907 (s) cm^{-1}. UV−vis (in THF): $\lambda_{max} =$ 393 and 511 nm. $T_g = 65$ °C; $M_w > 528\,000$ as measured by GPC (gel permeation chromatography) with a light-scattering detector. (Some photochemical decomposition occurred during the molecular weight measurement so this M_w value is a lower limit.)

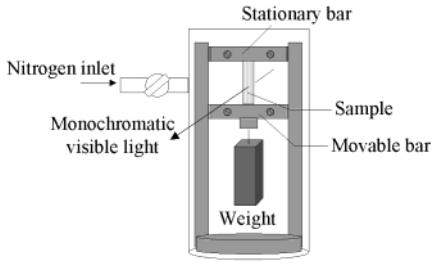

Figure 1. Device used to stress polymer films anaerobically during irradiation. The apparatus is enclosed in a glass container that is filled with nitrogen.

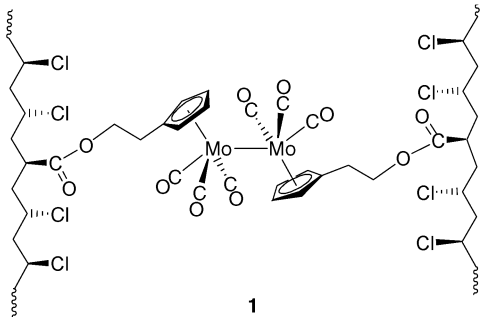

1

Preparation of Polymer 2 (Polymer 1 with 20 wt % DOP). The procedure for polymer **1** was followed except that, after the filtration to remove the triethylamine hydrochloride salt, DOP (0.08 g, 20 wt % of acyl chloride-activated PVC) was added to the filtrate with stirring. Half of the solvent was then evaporated and the concentrated solution was poured onto the Teflon-coated pan to form a liquid film. The film was dried in the glovebox for 2 days, and the final solvent residue was removed in vacuo. IR (of thin film): ν(C═O), 1770 (m) and 1730 (s) cm^{-1} (the intensities were skewed by DOP); ν(C≡O) of $[-Mo_2(CO)_6]$, 2005 (m), 1950 (s), and 1907 (s) cm^{-1}. UV−vis (in THF): $\lambda_{max} = 393$ and 511 nm. $T_g = 22$ °C.

Photodegradation of the Polymers under Stress. In a glovebox, the polymer films were cut into rectangular strips (30 mm length, 5−6 mm width, and about 0.04 mm thickness) and mounted in the equipment shown in Figure 1. The thickness was measured by an electronic digital caliper (Control Co.). Each sample was measured three times; the average value was used for the calculation. The error is ±0.005 mm. Stress was applied by hanging weights from the film. The apparatus was removed from the glovebox and then irradiated ($\lambda = 546$ nm) in an Oriel Merlin system equipped with a 200 W high pressure mercury arc lamp. The thin films of polymers **1** and **2** were photochemically reactive ($\lambda = 546$ nm) in the absence of oxygen. Infrared spectroscopic monitoring of the photochemical reaction showed the disappearance of the ν(C≡O) bands of $[-Mo_2(CO)_6]$ at 2005, 1950, and 1907 cm^{-1} and the appearance of bands attributed to the $[-Mo(CO)_3Cl]$ unit at 2048 and 1967 cm^{-1}. The data collected in the first 12 min of irradiation were used to calculate the quantum yield.

Scheme 2. Generalized Reaction Scheme Showing Photolysis of a Metal−Metal Bond along the Backbone in a Polymer

i) ~~M−M~~ $\underset{k_{recombination}}{\overset{\phi_{homolysis}}{\rightleftharpoons}}$ ~~M• + •M~~

ii) ~~M• + •M~~ $\xrightarrow{X = trap}$ 2 ~~M−X~~

The quantum yield[44] was calculated using the following equation:

$$\phi = \frac{-\int_{c_0}^{c_t} \frac{dc}{1 - 10^{-\epsilon l c}}}{I_0 \cdot t} \cdot A \cdot l$$

where I_0 is the incident intensity of the light ($\lambda = 546$ nm) in units of Einstein/s, l is the thickness (cm) of the sample film, A is the area (cm^2) exposed to the light, and t is 720 s. The degradation rate was calculated from the change in absorbance vs time using the system previously described.[44]

Results and Discussion

Theories of Stress-Induced Photodegradation. Mechanistic hypotheses to explain stress-accelerated photodegradation fall into three main categories. In one category, it is proposed that stress leads to an increase in the quantum yields for bond photolysis; i.e., it is proposed that $\phi_{homolysis}$ increases with stress (Scheme 2). The second category attributes the increased degradation rates to a decrease in the efficiency of radical recombination following homolysis; i.e., $k_{recombination}$ is proposed to decrease as stress increases. The third category attributes the effects of stress to changes in the rates of reactions that occur after formation of the radicals, i.e., to changes in the rate of the radical trapping reactions (eq ii in Scheme 2). The salient points of these theories are outlined in the following sections.

Stress-Induced Changes in $\phi_{homolysis}$: the Plotnikov Hypothesis. For a direct photochemical bond cleavage, the photochemical step in Scheme 2 labeled "$\phi_{homolysis}$" can be broken down into the nominal set of elementary steps shown in eq 2. (The asterisk in eq 2 is used to indicate an excited state of the molecule.)

$$\sim\!M\!-\!M\!\sim \underset{k_r}{\overset{h\nu}{\rightleftharpoons}} \left[\sim\!M\!-\!M\!\sim\right]^* \xrightarrow{k_{homolysis}} \sim\!M\bullet + \bullet M\!\sim \qquad (2)$$

Equation 3 shows the value of $\phi_{homolysis}$ in terms of the rate constants in eq 2.

$$\phi_{homolysis} = \frac{k_{homolysis}}{k_{homolysis} + k_r} \qquad (3)$$

Clearly, if stress affects either k_r or $k_{homolysis}$ then $\phi_{homolysis}$ will vary with stress. No theoretical studies have investigated the effect of stress on k_r, but Plotnikov derived a theory for the stress dependence of $k_{homolysis}$.[33] His quantitative hypothesis attributes the increase in degradation rates with applied stress to a decrease in the activation barrier for bond dissociation in the excited state. The relevant equation is given in the Supporting Information, and the predicted relationship of quantum yield to stress is shown in Figure 2a.

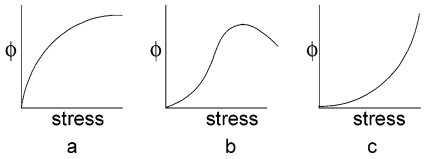

Figure 2. Plots of quantum yield for degradation vs stress according to (a) the Plotnikov equation, (b) the DRRE hypothesis, and (c) the Zhurkov equation.

Stress-induced Changes in $k_{recombination}$: The "Decreased Radical Recombination Efficiency" (DRRE) Hypothesis. Busfield,[14] Rogers,[15,34] Baimuratov,[35] and others[36] proposed explanations for stress effects that are based on decreases in radical recombination efficiencies in stressed systems. In their models (which are reasonably similar, so they are combined here for ease of discussion), the effect of stress is divided into four stages (see Figure S1 in the Supporting Information). Stage one represents the low stress domain. In this stage, there is only slight deformation of the original polymer structure and the rate of photodegradation is not greatly affected. In stage two, higher stress causes significant morphological changes, including the straightening of the polymer chains in the amorphous regions. When bonds in the taut tie molecules are cleaved by light, the probability of radical recombination is decreased relative to nonstressed samples because entropic relaxation drives the radicals apart and prevents their efficient recombination. At slightly higher stresses (stage three), the chains are not only straightened but "stretched", and recoil aids in their separation. According to this model, the diminished ability of the radicals to recombine is the primary reason that tensile stress will increase the rate of photodegradation. An increased separation leads to slower radical−radical recombination, which increases the probability of radical trapping and thus of degradation. Finally, in stage four, a strong stress is present which gives the polymer a fibrillar structure with a higher degree of orientation and crystallinity. Diffusion in a crystalline structure is retarded relative to the amorphous material, and the rate of degradation is expected to decrease because of decreased movement apart of the radicals. In summary, the DRRE hypothesis predicts that tensile stress will initially increase the quantum yield of degradation and then further increases in stress will decrease the quantum yield (Figure 2b).

Stress-Induced Changes in the Rates of Radical Reactions after Radical Formation. The effect of stress on the rates and efficiencies of reactions that occur after radical formation is complicated. Examples have been noted where the rates decrease because of decreased oxygen diffusion[8,9] in the stressed (more ordered) sample.[37] In other systems, it has been suggested that the important point is that stress changes the conformations of the C−C bonds in the polymer chains;[38−40] depending on the system either a rate decrease[38−40] or a rate increase[41] can occur. The quantitative relationship of quantum yields to stress in such cases is generally considered to be given by the so-called Zhurkov equation, as discussed in the next section.

The Zhurkov Equation. The effect of stress on the *thermal* degradation rates of polymers can be fitted to an empirical Arrhenius-like equation that is attributed

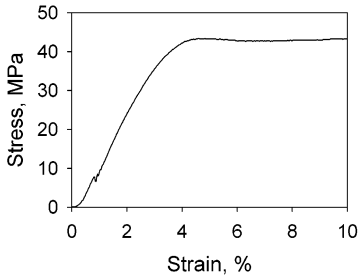

Figure 3. Stress−strain curve for polymer **1**.

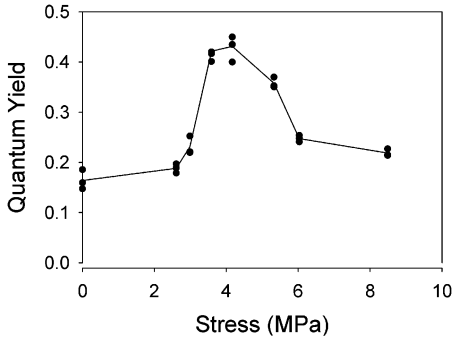

Figure 4. Quantum yields for degradation of **1** vs applied tensile stress. The results of three independent measurements at each stress are shown.

to Zhurkov:[42] rate = $A \exp[-(\Delta G - B\sigma)/RT]$ where ΔG is an "apparent" activation energy, σ is the stress, and A and B are constants. It has been suggested[2] that an equation similar to the Zhurkov equation might apply in photodegradation: $\phi_{obs} = A \exp[-(\Delta G - B\sigma)/RT]$. The Zhurkov equation is empirical and does not fall strictly into any of the three mechanistic categories discussed above because it deals with an "effective" activation energy, which (in the case of a photochemical reaction) is a composite of the activation barriers for the $\phi_{homolysis}$, $k_{recombination}$, and $k_{trapping}$ steps. The relationship of quantum yield to stress for a system that follows the Zhurkov hypothesis is shown in Figure 2c.

Quantum Yields as a Function of Stress for Polymer 1. Thin films of polymer **1** were stressed by hanging weights of known mass from one end of the film as shown in Figure 1.[43] The stress was varied from 0 to 10 MPa. Note that the maximum applied stress (10 MPa) is about 20% of the yield stress in commercial PVC. Also note that the range of stress investigated fell in the initial part of the elastic stage, as indicated by the stress−strain curve (Figure 3). At each stress, the quantum yield of Mo−Mo disappearance was calculated from the data collected in the first 12 min of irradiation using the system previously described.[44] Figure 4 is a plot of the quantum yield for the degradation of **1** as a function of stress. Note that the quantum yields increased with increasing stress, reached a maximum, and then decreased. As discussed above, such a plot is predicted by the DRRE hypothesis (Figure 2b).

Evidence for an Increase in Order with Increasing Stress: Infrared Spectroscopy. A key tenet of the DRRE hypothesis is that stress eventually causes ordering of the amorphous polymer chains and this ordering causes a decrease in the quantum yields of the polymer decomposition. Infrared spectroscopy provides a convenient way to monitor changes in crystallinity as a function of stress. Bands in the 1400−1450, 1200−1285, and 580−720 cm^{-1} regions have been assigned to

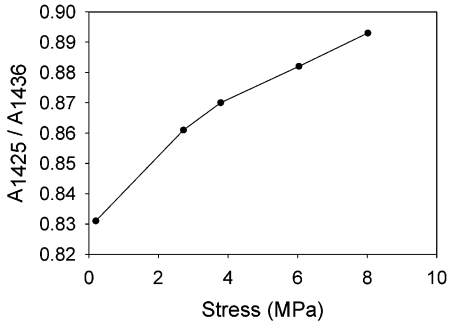

Figure 5. Ratio of A_{1425}/A_{1436} vs applied tensile stress for polymer **1**.

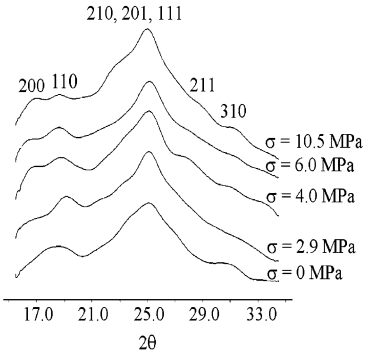

Figure 6. Wide-angle X-ray diffraction patterns of polymer **1** at various stresses.

the CH_2 bending, CH bending, and C−Cl stretching modes of PVC, respectively.[45,46] As discussed by a number of authors, the frequencies of these modes are sensitive to chain conformation and crystallinity.[47] For example, the CH_2 bending modes at 1436 and ≈1425 cm^{-1} have been assigned to amorphous and crystalline PVC, respectively, and therefore the ratio of the band intensities (A_{1425}/A_{1436}) can be used to give a relative measure of crystallinity.[49] Likewise, the A_{1253}/A_{1240} ratio has also been used to estimate relative changes in crystallinity.[50] Similarly, it is generally agreed that the band at 610−615 cm^{-1} arises from a C−Cl stretch in amorphous regions and the band at 635−638 cm^{-1} arises from C−Cl stretching of a long syndiotactic sequence in crystalline regions. Therefore, the absorbance ratio A_{637}/A_{615} can also be used to measure relative amounts of crystallinity in stressed PVC. Finally, the band at 604 cm^{-1} is characteristic of long, zigzag, planar, syndiotactic sequences in crystalline PVC, and the 615 cm^{-1} band is characteristic of short, planar syndiotactic segments in amorphous PVC. Thus, the absorbance ratio A_{604}/A_{615} can also be used to measure relative amounts of crystallinity in stressed PVC.

Figure 5 shows the effects of applied stress on the crystallinity index A_{1425}/A_{1436} as a function of stress for polymer **1**. Plots of A_{1253}/A_{1240}, A_{637}/A_{615}, and A_{604}/A_{615} as a function of stress are shown in the Supporting Information as Figures S2−S4. In each case, the value of these indices increased with increasing stress, a result consistent with increased stress causing increased crystallinity.[51]

Evidence for an Increase in Order with Increasing Stress: X-ray Diffraction. X-ray diffraction was also used to evaluate the crystallinity of polymer **1** thin films under stress. Figure 6 shows the X-ray diffraction patterns for polymer **1** at various stresses. (The peaks of crystalline reflection are based on assignments in

previous reports.[52−54]) As shown by Maddams,[55] the (*h*00) and (*hk*0) type reflections in the 14−20° 2θ region are a measure of two-dimensional order perpendicular to the chain direction, while the (*hkl*) type reflections in the 20−30° 2θ region are a measure of three-dimensional order. Note that for a stress of 0 MPa, the diffraction pattern showed one broad diffraction maximum in the 16−18° 2θ region and another maximum at about 25° 2θ. These data are similar to those found in commercial samples of PVC, which contain just a few percent crystallinity, suggesting that polymer **1** at 0 MPa likewise has just a small amount of crystallinity. The data show that with increasing stress on the film there was enhanced intensity in the 16−18° 2θ region, indicative of increased two-dimensional order perpendicular to the chain direction. More precisely, the intensity changes of the (200) and (110) reflections showed an increase in the lateral crystallite dimensions in stressed PVC. Note that the diffraction patterns are not completely reversible when the stress is removed after stretching the films to $\sigma >$ 4.2 MPa. This is likely attributable to stress-induced crystallization.

Effect of Stress on the Photodegradation of Polymer 2. The results above are consistent with the predictions of the DRRE hypothesis. Recall that, in this hypothesis, the initial effect of stress on the degradation efficiency is to separate the photogenerated radicals further from each other and thereby lower their recombination efficiency. At higher stresses, however, the stress induces enough order in the polymer chain to prevent radical separation, which increases their recombination efficiency and lowers the degradation efficiency. Additional mechanistic evidence consistent with the DRRE hypothesis was sought in order to confirm this interpretation on the role of stress, and for that reason the experiments described above were repeated with polymer **2** (plasticized polymer **1)**. Because chain movements are more facile in plasticized polymer, it was predicted that, at any given stress, the quantum yields for degradation should be higher (because it is easier for the radicals to separate from each other, which lowers their probability of recombination). In addition, the maximum in the curve shown in Figure 4 should occur at a lower stress because chain alignment is easier.

Polymer **2** was made by mixing **1** with dioctyl phthalate (DOP).[56,57] As expected, the presence of the plasticizer decreased the glass transition temperature (T_g) of the polymer from 65 °C to <25 °C. As likewise expected, the DOP plasticizer resulted in a decrease in the tensile strength and yield stress and a longer elongation compared to polymer **1** (Figure S5). A plot of quantum yield for degradation vs tensile stress for polymer **2** is shown in Figure 7. Although there is considerably more scatter in this plot than that for polymer **1**, it is apparent that these results also match the predictions of the DRRE hypothesis; i.e., stress initially causes an increase in degradation efficiency to some maximum value, at which point the quantum yields start to decrease. Note that, for a given stress, the quantum yields of degradation are higher for polymer **2** than for polymer **1**. In addition, the maximum in the curve occurs at a lower stress compared to the plot in Figure 4 for polymer **1**. Both of these results are consistent with the predictions made in the preceding paragraph concerning the effect of plasticizer, and this is taken as additional evidence in support of the DRRE hypothesis.

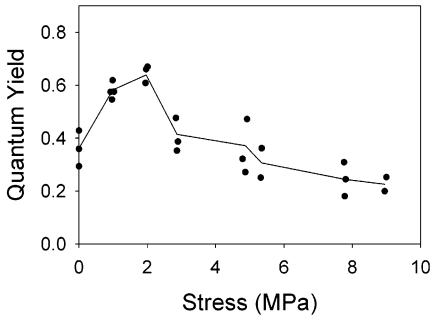

Figure 7. Quantum yields for degradation of **2** vs applied tensile stress. The results of several independent measurements at each stress are shown.

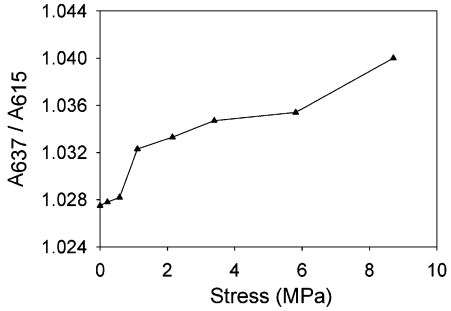

Figure 8. Ratio of A_{637}/A_{615} vs applied tensile stress for polymer **2**.

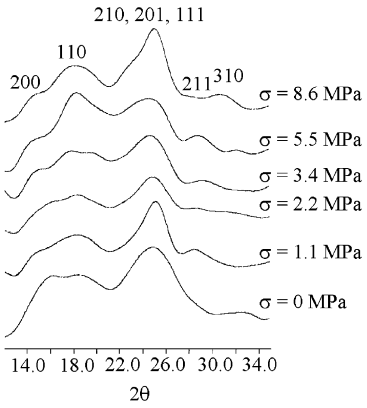

Figure 9. Wide-angle X-ray diffraction patterns of polymer **2** at various stresses.

Evidence for an Increase in Order with Increasing Stress in Polymer 2: Infrared Spectroscopy and X-ray Diffraction. The infrared spectrum of **2** has overlapping PVC and DOP bands in the CH_2 bending and CH bending regions (Figure S6; also see Table S1). Thus, it was not possible to use the A_{1425}/A_{1436} and A_{1253}/A_{1240} absorbance ratios to track changes in the relative crystallinity of the sample. Attempts to subtract the contribution of DOP from the plasticized polymer spectrum, as described in a previous study by Koenig,[49] did not give satisfactory results in this case. However, it was possible to use the A_{637}/A_{615} ratio as a cystallinity index. This ratio is plotted as a function of stress in Figure 8. Note the general increase in this ratio as stress is increased, indicative of increased crystallinity with increasing stress.

X-ray diffraction patterns of polymer **2** were also consistent with increased cystallinity with increased stress (Figure 9). Note that polymer **2** is not completely amorphous at zero applied stress but rather slightly crystalline in nature. (This is indicated by the rather

well-defined (110) and (200) reflections at 0 MPa.) As explained by Alfrey, the internal structure of plasticized PVC consists of two separate disperse phases: crystalline regions containing only PVC segments and regions containing amorphous PVC and plasticizer.[58] Note that increasing stress increases the intensities of the (110) and (200) reflections, indicative of increasing two-dimensional order. (Guerrero[54] cites work by Vickers showing that the (110) reflection is especially sensitive (more than the (200) reflection) to small rotations of the molecules along their long axis. Mammi[53] and Lebedev[59] showed that the 18° 2θ peak (i.e., the (110) reflection) is characteristic of a mesomorphous or nematic phase with some order in the parallel arrangement of the chains.) Note there are also changes in the intensity of the 25° 2θ reflection as the polymer is stressed. This change is indicative of an increase in the three-dimensional order of the polymer film.[55] Note in Figure 9 that the 18° reflections are initially less intense than the peak at 25° 2θ, but increasing the stress increased the relative intensity of the 18° peaks until at 5.5 MPa the 18° peaks are more intense than the 25° peak. Further increasing the stress to 8.6 MPa then increased the relative intensity of the 25° peak. This sequence shows that two-dimensional order is established first, followed by three-dimensional order, as expected.

Key Insights and Conclusions. The results presented above are consistent with the predictions of the DRRE hypothesis. According to this hypothesis, the initial effect of stress on the degradation efficiency is to separate the photogenerated radicals further from each other than in the absence of stress and thereby lower their recombination efficiency. At higher stresses, however, the stress induces enough order in the polymer chains to inhibit radical separation, which increases their recombination efficiency and lowers the degradation efficiency. Although it is tempting to generalize these results to other polymers and to other degradation mechanisms (photooxidative degradations, in particular) it is prudent to be cautious. For example, in a photooxidation reaction, the downturn in efficiency with higher stress may be caused by the development of microcracks and fissures, which act to release the stress. Or, perhaps the k_r term in eqs 2 and 3, generally assumed to be stress independent, is in fact stress dependent, and this caused the downturn. Work in our lab is continuing to address these issues.

Acknowledgment is made to the National Science Foundation (DMR-0096606) for the support of this work.

Supporting Information Available: Text giving the Plotnikov equation referred to in the paper, Figure S1, the mechanistic origin of the decrease in radical−radical recombination in a stretched polymer (the DRRE hypothesis), Figure S2, the ratio of A_{1253}/A_{1240} vs applied tensile stress for polymer **1**, Figure S3, the ratio of A_{637}/A_{615} vs applied tensile stress for polymer **1**, Figure S4, the ratio of A_{604}/A_{615} vs the applied tensile stress for polymer **1**, Figure S5, the stress−strain curve of polymer **2**, Figure S6, infrared spectra from 500 to 1500 cm^{-1} for polymer **1**, polymer **2**, and DOP, and Table S1, summary of DOP infrared frequencies relevant to the determination of crystallinity in polymer **2**. This material is available free of charge via the Internet at http://pubs.acs.org.

References and Notes

(1) Grassie, N.; Scott, G. *Polymer Degradization and Stabilization*; Cambridge University Press: New York, 1985.
(2) White, J. R.; Rapoport, N. Y. *Trends Polym. Sci.* **1994**, *2*, 197−202.
(3) Guillet, J. *Polymer Photophysics and Photochemistry: An Introduction to the Study of Photoprocesses in Macromolecules*; Cambridge University Press: New York, 1985.
(4) Rabek, J. F. *Mechanisms of Photophysical Processes and Photochemical Reactions in Polymers*; Wiley: New York, 1987.
(5) O'Donnell, B.; White, J. R. *J. Mater. Sci.* **1994**, *29*, 3955−3963.
(6) O'Donnell, B.; White, J. R. *Polym. Prepr. (Am. Chem. Soc., Div. Polym. Chem.)* **1993**, *34*, 137−138.
(7) Tong, L.; White, J. R. *Polym. Degrad. Stab.* **1996**, *53*, 381−396.
(8) Baumhardt-Neto, R.; De Paoli, M. A. *Polym. Degrad. Stab.* **1993**, *40*, 59−64.
(9) Baumhardt-Neto, R.; De Paoli, M. A. *Polym. Degrad. Stab.* **1993**, *40*, 53−58.
(10) Schoolenberg, G. E.; Vink, P. *Polymer* **1991**, *32*, 432−437.
(11) Kelly, C. T.; Tong, L.; White, J. R. *J. Mater. Sci.* **1997**, *32*, 851−861.
(12) O'Donnell, B.; Qayyum, M. M.; Tong, L.; White, J. R. *Polym. Prepr. (Am. Chem. Soc., Div. Polym. Chem.)* **1993**, *34*, 211−212.
(13) Kelly, C. T.; White, J. R. *Polym. Degrad. Stab.* **1997**, *56*, 367−383.
(14) Busfield, W. K.; Monteiro, M. J. *Mater. Forum* **1990**, *14*, 218−223.
(15) Benachour, D.; Rogers, C. E. *ACS Symp. Ser.* **1981**, *151*, 263−274.
(16) Igarashi, M.; DeVries, K. L. *Polymer* **1983**, *24*, 1035−1041.
(17) Huvet, A.; Philippe, J.; Verdu, J. *Eur. Polym. J.* **1978**, *14*, 709−713.
(18) Busfield, W. K.; Taba, P. *Polym. Degrad. Stab.* **1996**, *51*, 185−196.
(19) Thominette, F.; Verdu, J. *Polym. Prepr. (Am. Chem. Soc., Div. Polym. Chem.)* **1994**, *35*, 971−972.
(20) Tupikov, V. I.; Khatipov, S. A.; Stepanov, V. F. *Phys. Chem. Mater. Treatment* **1997**, *31*, 32−36.
(21) Igarashi, M.; DeVries, K. L. *Polymer* **1983**, *24*, 769−782.
(22) Matsui, H.; Arrivo, S. M.; Valentini, J. J.; Weber, J. N. *Macromolecules* **2000**, *33*, 5655−5664.
(23) Nichols, M. E.; Gerlock, J. L.; Smith, C. A. *Polym. Degrad. Stab.* **1997**, *56*, 81−91.
(24) Nguyen Truc Lam, H.; Rogers, C. E. *Polym. Mater. Sci. Eng.* **1987**, *56*, 589−592.
(25) Tyler, D. R. *Coord. Chem. Rev.* **2003**, *246*, 291−303.
(26) Geuskens, G. *Compr. Chem. Kinet.* **1975**, *14*, 333−424.
(27) Cunliffe, A. V.; Davis, A. *Polym. Degrad. Stab.* **1982**, *4*, 17−37.
(28) Malik, J.; Hrivik, A.; Tuan, D. Q. *Adv. Chem. Ser.* **1996**, *249*, 455−471. See page 459 in particular.
(29) Tenhaeff, S. C.; Tyler, D. R. *Organometallics* **1991**, *10*, 473−482.
(30) Tenhaeff, S. C.; Tyler, D. R. *Organometallics* **1991**, *10*, 1116−1123.
(31) Tenhaeff, S. C.; Tyler, D. R. *Organometallics* **1992**, *11*, 1466−1473.
(32) Chen, R.; Yoon, M.; Smalley, A.; Johnson, D. C.; Tyler, D. R. *J. Am. Chem. Soc.* **2004**, *126*, 3054−3055.
(33) Plotnikov, V. G. *Dokl. Akad. Nauk SSSR* **1988**, *301*, 376−379.
(34) Nguyen, T. L.; Rogers, C. E. *Polym. Mater. Sci. Eng.* **1985**, *53*, 292−296.
(35) Baimuratov, E.; Saidov, D. S.; Kalontarov, I. Y. *Polym. Degrad. Stab.* **1993**, *39*, 35−39.
(36) Shlyapikov, Y. A.; Kiryushkin, S. G.; Marin, A. P. *Antioxidative Stabilization of Polymers*; Taylor and Francis: Bristol, PA, 1996.
(37) Rabello, M. S.; White, J. R. *Polym. Degrad. Stab.* **1997**, *56*, 55−73.
(38) Bellenger, V.; Verdu, J.; Martinez, G.; Millan, J. *Polym. Degrad. Stab.* **1990**, *28*, 53−65.
(39) Rapoport, N. Y.; Zaikov, G. E. *Eur. Polym. J.* **1984**, *20*, 409−414.
(40) Rapoport, N. Y.; Shibryaeva, L. S.; Zaikov, V. E.; Iring, M.; Fodor, Z.; Tudos, F. *Polym. Degrad. Stab.* **1985**, *12*, 191−202.
(41) Castillo, F.; Martinez, G.; Sastre, R.; Millan, J.; Bellenger, V.; Gupta, B. D.; Verdu, J. *Polym. Degrad. Stab.* **1990**, *27*, 1−11.
(42) Zhurkov, S. N.; Zakrevskii, V. A.; Korsukov, V. E.; Kuksenko, V. S. *J. Polym. Sci., Polym. Phys. Ed.* **1972**, *10*, 1509−1520.

(43) The stress on the film was calculated using the equation σ (MPa) = {M (kg) × 9.8 (m/s^2)}/{w (mm) × l (mm)}, where M is the total weight hanging from the end of the film, w is the width of film, and l is its thickness.
(44) The apparatus used to monitor the reaction and monitor the light intensity for quantum yields is described in: Lindfors, B. E.; Nieckarz, G. F. Tyler, D. R.; Glenn, A. G. *J. Photochem. Photobiol. A: Chem.* **1996**, *94*, 101−105. The quantum yield procedure is essentially the same as described in that paper except that the samples in the current study were thin films rather than solution phase samples. Note that the apparatus can irradiate the film and monitor the reaction simultaneously, and hence the sample does not move during the irradiation (i.e., there is no need to remove the sample from the light beam to put it in a spectrophotometer). The bane of solid-state quantum yield measurements is repositioning the sample in its original position after each spectroscopic analysis. The apparatus used in this study was designed to circumvent this problem.
(45) Krimm, S.; Folt, V. L.; Shipman, J. J.; Berens, A. R. *J. Polym. Sci., A* **1963**, *1*, 2621−2650.
(46) Tasumi, M.; Shimauouchi, T. *Spectrochim. Acta* **1961**, *17*, *73*1−754.
(47) The molecular structure of PVC is complex. Although amorphous to a considerable extent, it contains different types of crystallites, depending on its thermal history and processing conditions. Commercial PVC is known to possess a small amount of crystallinity (no more than 10%). A number of studies have attempted to use infrared spectroscopy to quantify the amount of crystallinity and to provide useful information about chain conformations in the crystalline phase and amorphous phases. The study by Zerbi, Ciampelli, and Zamboni is representative.[48] These workers divided the infrared bands of PVC into three types. The first type consists of bands that characterize the configuration and conformation of the sample; these bands are always present, whatever the physical state of the sample. Most of the bands in the carbon−chlorine stretching region are of this type, at least for commercial PVC. The second type of band is associated with long stereoregular chain segments. These bands are present even in noncrystalline samples, which proves they are not due to the crystalline phase of PVC. The third type consists of bands that are characteristic of crystalline regions, and consequently their intensity can be used to assess the amount of crystallinity. It is interesting to note that the crystalline bands have peaks split into two components, caused by the interactions between neighboring chains in the crystal unit cell. The two bands cannot be observed simultaneously because one component of each pair is infrared active and the other one Raman active.
(48) Zerbi, G.; Ciampelli, F.; Zamboni, V. *Conference on the Vibrational Spectra of High Polymers*; Natta, G., Zerbi, G., Eds.; Interscience: New York, 1964; p 3.
(49) Tabb, D. L.; Koenig, J. L. *Macromolecules* **1975**, *8*, 929−934.
(50) Witenhafer, D. E. *J. Macromol. Sci., Phys.* **1970**, *4*, 915−929.
(51) The ratio A_{604}/A_{615} increased with increasing stress, especially in the range 0−6 MPa. As mentioned previously, the bands at 604 and 615 cm^{-1} are characteristic of long and short, planar syndiotactic segments, respectively. Thus, the amount of long, planar syndiotactic segments increased with increased stress.
(52) Natta, G.; Corradini, P. *J. Polym. Sci.* **1956**, *20*, 251−266.
(53) Mammi, M.; Nardi, V. *Nature (London)* **1963**, *199*, 247−249.
(54) Guerrero, S. J.; Veloso, H.; Randon, E. *Polymer* **1990**, *31*, 1615−1622.
(55) Baker, C.; Maddams, W. F.; Preedy, J. E. *J. Polym. Sci., Polym. Phys. Ed.* **1977**, *15*, 1041−1054.
(56) DOP is commonly used as a plasticizer in PVC processing to reduce the processing temperature. Here, 20 wt % DOP content was chosen because it gave a material with T_g less than room temperature.[57.]
(57) Beirnes, K. J.; Burns, C. M. *J. Appl. Polym. Sci.* **1986**, *31*, 2561−2567.
(58) Alfrey, T., Jr.; Wiederhorn, N.; Stein, R.; Tobolsky, A. *J. Colloid Sci.* **1949**, *4*, 211−227.
(59) Lebedev, V. P.; Okladnov, N. A.; Shlykova, M. N. *Polym. Sci. U.S.S.R.* **1967**, *9*, 553.

MA0496302